Direct Detection of Iron Clusters in L Ferritins through ESI MS Experiments

Lara Massai,[a,‡] Silvia Ciambellotti,[a,b,c,‡] Lucrezia Cosottini,[a,b,c] Luigi Messori,[a,*] Paola Turano,[a,b,c,*] Alessandro Pratesi[d]

Human cytoplasmic ferritins are heteropolymers of H and L subunits containing a catalytic ferroxidase center and a nucleation site for iron biomineralization, respectively. Here, ESI-MS successfully detected labile metal-protein interactions revealing the formation of tetra and octa-iron clusters bound to L subunits, as previously underscored by X-ray crystallography.

Ferritin is a key protein in the metabolism of iron.[1] With its 24-mer nanocage structure hosting an internal cavity of 8 nm, ferritin stores iron under the form of a ferric biomineral and makes it readily bioavailable for cellular uses. At the same time, by sequestering free iron, it prevents the formation of harmful reactive oxygen species (ROS) that may be generated through Fenton chemistry. Ferritin acts as a buffer against iron deficiency and iron overload. In humans, ferritins are found intracellularly in the cytosol,[2] in the mitochondria,[3] in the nucleus,[4–6] and extracellularly in serum[7] and cerebrospinal fluid.[8] Cytoplasmic ferritins are heteropolymers with a variable ratio of H (heavy) and L (light) subunits, depending on the type of tissue and cell as well as on the actual physio-pathological conditions. H subunits contain a catalytic ferroxidase site for the fast oxidation of Fe^{2+} to Fe^{3+} by O_2. L subunits, sharing 53% homology with the H ones (Figure S1), lack this catalytic center but facilitate the (relatively slow) biomineral formation at nucleation sites situated on the inner cage surface.

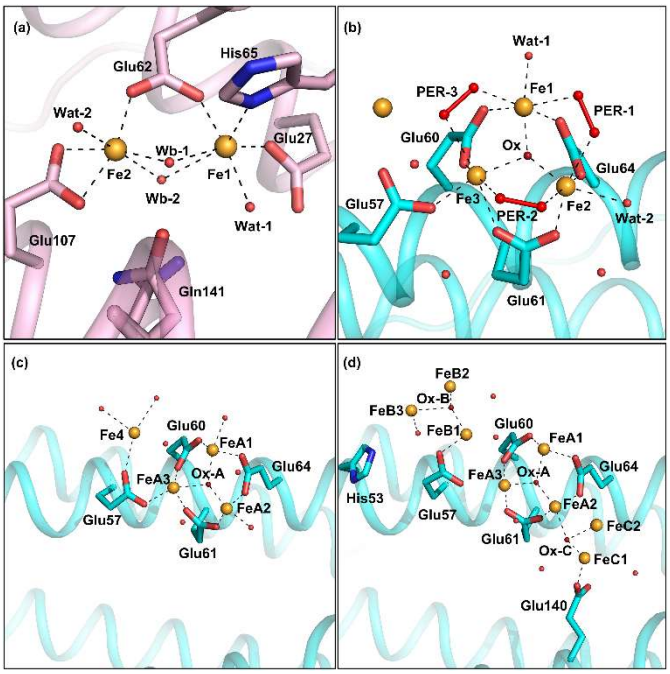

Fig. 1. a) Dinuclear ferroxidase site of human H ferritin (PDB id: 4ZJK);[9] b) nucleation site of human L ferritin (PDB id: 5LG8)[10] occupied by a tri-nuclear iron cluster; c) and d) 4- and 8-nuclear cluster on the inner surface of human L ferritin (PDB id: 6TSJ, 6TSF),[11] respectively. For an exact location of these metal centers inside the HuHf and HuLf see Figure S2.

Time-lapse anomalous X-ray diffraction studies on recombinant homopolymeric H and L ferritins (HuHf and HuLf, respectively) permitted to capture iron-binding events occurring at a series of sites throughout the nanocages,[9–11] including the ferroxidase center in catalytic ferritins and the nucleation site of L ferritins (Figure 1). Iron bound to the nucleation sites was observed using two different experimental procedures. The freezing of L ferritin crystals after exposure to a ferrous solution allowed the observation of a (μ³-oxo)Tris[(μ²-peroxo)(μ²-glutamato-κO:κO')](glutamato-κO)(diaquo)triiron(III) cluster, with Glu60, Glu61, and Glu64 as iron ligands and with Glu57 shuttling a

[a] *Department of Chemistry "Ugo Schiff", University of Florence, Via della Lastruccia 3-13, 50019 Sesto Fiorentino (FI), Italy.*
Email: luigi.messori@unifi.it
[b] *Magnetic Resonance Center (CERM), University of Florence, Via Luigi Sacconi 6, 50019 Sesto Fiorentino (FI), Italy.*
Email: turano@cerm.unifi.it
[c] *Consorzio Interuniversitario Risonanze Magnetiche di Metallo Proteine (C.I.R.M.M.P.), Via Luigi Sacconi 6, 50019 Sesto Fiorentino (FI), Italy.*
[d] *Department of Chemistry and Industrial Chemistry (DCCI), University of Pisa, Via Giuseppe Moruzzi 13, 56124 Pisa, Italy.*
‡ These authors contributed equally to this work.
Electronic Supplementary Information (ESI) available: [Additional experimental details, preparation of ferritin samples, structural details of nucleation and ferroxidase sites, multiple sequence alignment, additional ESI mass spectra, peak assignments through experimental and theoretical isotopic patterns (PDF)]. See DOI: 10.1039/x0xx00000x

fourth incoming iron ion toward the cluster (Figure 1b).[10] Repeating the experiment with Fe^{3+} diffusion led to the observation of a similar species, lacking the peroxo moieties, and with Glu57 bridging one iron ion of the (μ^3-oxo) center and a fourth iron ion (Figure 1c).[11] Under these experimental conditions, at longer exposure times, it was possible to observe the growth of this initial cluster to produce an octanuclear species where the additional iron ions are poorly interacting with the protein side chains (Figure 1d).[11] These clusters are proposed to represent the initial seeds for the biomineral growth, which recent data suggest to proceed via an inner-surface assisted process.[12] The cluster formation is completely quenched in the triple mutant E60AE61AE64A.

We wondered whether the formation of these iron clusters might be detected also in solution and confirmed through an independent method. Accordingly, we explore here whether ESI MS is a suitable tool to characterize the interactions of iron ions with the ferritin nanocage and to reveal the formation of the above clusters in HuLf and -possibly- of the dinuclear metal centre at the ferroxidase sites of HuHf, after iron upload in ferritin solutions.

Indeed, ESI mass spectrometry is an emerging and powerful method to study metal-protein interactions.[13–16] In particular, the use of soft ionization methods offers the opportunity to conserve the relatively weak metal to protein coordination bonds in the gas phase.[17–19] A few ESI MS studies of apo-ferritin were previously reported, including human ferritin[20,21] and horse spleen ferritin.[22] The latter is a natural heteropolymer with a H/L ratio of 10/1 and was analyzed in its commercial form, showing some iron contamination. While the detection of the 24-mer cage is quite problematic and challenging from the technical point of view owing to its exceedingly large size (ca. 480 kDa),[23] detection of the monomeric species is afforded quite straightforwardly, as demonstrated here by the ESI mass spectra recorded on human H and L (wild-type and triple mutant) ferritins (see below).

To prove the ability of ferritins to mediate the growth of the Fe clusters, the three studied ferritins, i.e. HuHf, HuLf and its E60AE61AE64A variant, were exposed to ferrous salts (the detailed procedure is reported in the Supporting Information). Briefly, all ferritins were deprived of iron taken from the growth medium during their expression in *E. coli*, through extensive dialysis in the presence of reductant and chelating agents. The resulting apo proteins were rapidly mixed after the addition of aliquots, equal to 350 Fe^{2+} per cage, taken from a stock fresh-prepared ferrous sulfate solution (in 1 mM HCl to prevent instantaneous iron oxidation).[24] After 2h of incubation at room temperature, the biomineralization process was carried out by storing the ferritin samples overnight at 4 °C. Then,

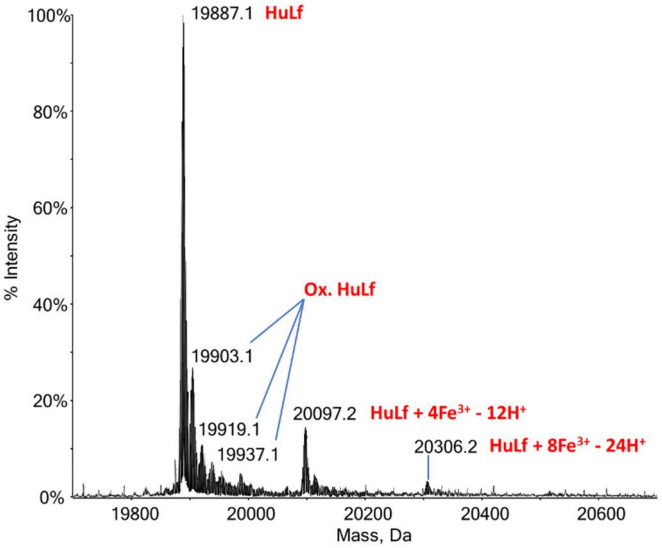

Fig. 2. Deconvoluted ESI mass spectrum of HuHf 10^{-6} M loaded with 350 Fe^{2+} ions per protein cage in 2 mM ammonium acetate solution at pH 6.8; 0.5% v/v of formic acid was added just before infusion.

centrifugation and ultrafiltration steps were applied to remove precipitates and iron ions not taken up by ferritin cages. Afterwards, iron treated ferritin samples were buffer exchanged into ammonium acetate and characterized through high-resolution mass spectrometry. The use of ammonium acetate is necessary to maintain the native protein conformation even with a volatile and ESI-MS-friendly solution.

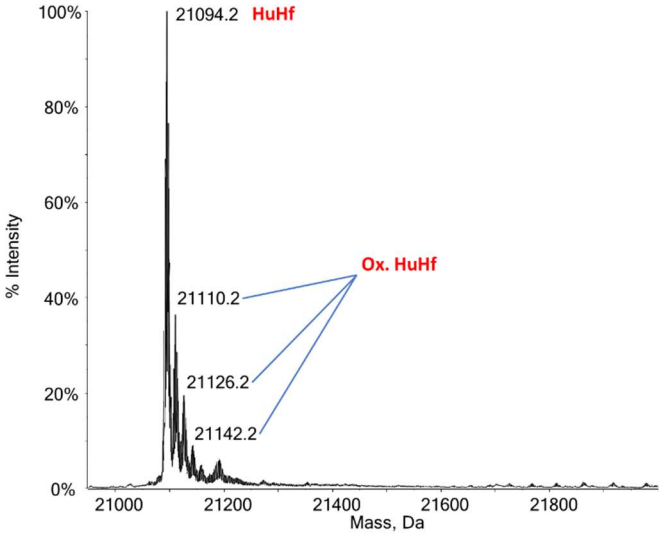

Fig. 3. Deconvoluted ESI mass spectrum of HuLf 10^{-6} M loaded with 350 Fe^{2+} ions per protein cage in 2 mM ammonium acetate solution at pH 6.8; 0.5% v/v of formic acid was added just before infusion.

Moreover, 0.5% v/v of formic acid was added just before infusion into the mass spectrometer with the aim to facilitate the protein protonation and to increase the signals intensity.

The spectrum of iron-loaded H ferritin, reported in Figure 2, shows an intense peak positioned at 21094.2 Da that is in agreement with the amino acid sequence of the ferritin heavy chain, deprived of the first Met residue (theoretical mass 21094.274 Da). A few additional small peaks are observed at 21110.2, 21126.2 and 21142.2 Da that arise from progressive oxidation in solution of the Met residues to methionine sulfoxide (see protein sequence in Figure S1).[25,26]

However, in this ESI mass spectrum, no signal attributable to Fe-containing clusters is detected. This finding is consistent with the labile nature of the iron at the catalytic ferroxidase centre of HuHf, and its lack of the nucleation site.[27,28] Analogously, the HuLf sample was incubated with the same amount of iron (350 iron ions per protein cage) and the respective ESI mass spectrum recorded (see Figure 3).

Notably, the mass spectrum of HuLf reveals an interesting feature at 20097.2 Da, whose mass nicely corresponds to four Fe^{3+} atoms bound to the protein.

The lack of signals for adducts of lower Fe/protein stoichiometry points out that the binding of these four iron atoms to HuLf is cooperative. The adduct assignments were confirmed by direct comparison of theoretical isotopic simulations with the respective measured isotopic patterns (see the Supporting Information).

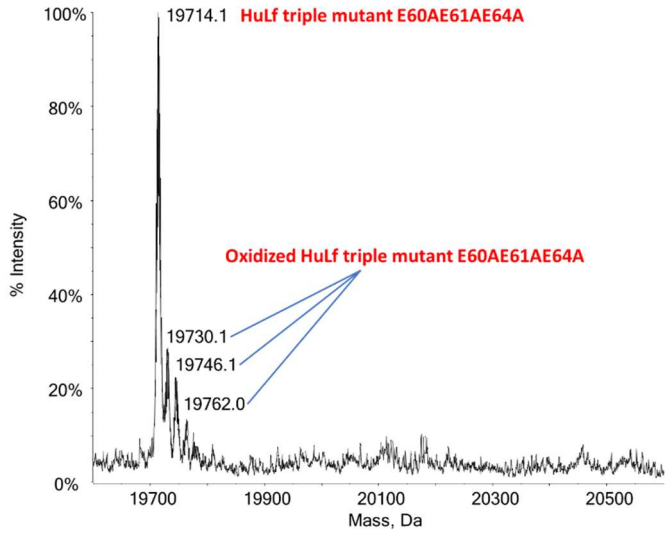

Fig. 4. Deconvoluted ESI mass spectrum of HuLf triple mutant E60AE61AE64A 10^{-6} M loaded with 350 Fe^{2+} ions per protein cage in 2 mM ammonium acetate solution at pH 6.8; 0.5% v/v of formic acid was added just before infusion.

As a further proof of the occurrence of cooperativity in iron binding to light chain ferritin, an additional peak of very low intensity can be detected at 20306.2 Da perfectly consistent with eight Fe^{3+} ions bound to ferritin.

The tetra- and octa- nuclear clusters are consistent with the X-ray data of Figure 1c,d and Figure S3 (clusters A, B and C). Instead, no peaks attributable to the transient tri-iron Z cluster of Figure S3 are observed.

In any case, the most intense peak in Figure 3 (19887.1 Da) remains that of the unreacted protein, deprived of the first methionine residue. Again, this signal is accompanied by those related to the various oxidized forms of the protein (19903.1, 19919.1 and 19937.1 Da). The presence of this group of signals belonging to the unreacted protein indicates a low degree of metalation of the HuLf chains under the applied ESI MS experimental conditions; quite surprisingly, this behavior turned out to be roughly independent of added iron concentration (in the range 72-480 Fe/cage).

Noteworthy, in no case the recorded ESI mass spectra showed signals of Fe/protein adducts with stoichiometry lower than 4:1.

To further prove the existence of iron clusters on the surface of HuLf, the same protein solution was incubated for further 15 min with a slight excess of ethylenediaminetetraacetic acid (EDTA); then, the ESI mass spectrum was again acquired. In this case, the spectrum showed only the signals of the protein in its apo form, while the signals of the iron clusters are lost (see the Supporting Information). This means that EDTA, owing to its pronounced metal chelating properties, is able to completely remove the iron ions from the L ferritin coordination site converting the protein to its apo form. On the ground of the previous crystallographic results,[10,11] we may well hypothesize that these iron atoms interact with residues located in the nucleation site.

With the aim to establish if these iron ions are bound to the protein portion containing Glu60, Glu61 and Glu64 residues, we further analyzed a HuLf E60AE61AE64A variant where the substitution of these Glu residues with Ala prevents iron binding, as demonstrated by iron-loaded structures solved by X-ray and kinetic analysis.[10,11] Again, the protein was exposed to 350 Fe^{2+} equivalents per cage, and the mass spectrum recorded (Figure 4).

As expected, due to the lack of the iron-binding Glu residues, the mutant form of HuLf is not able to assist the formation of iron clusters; hence the related peaks are not detected in the ESI mass spectrum. The only ESI MS signal is due to the unreacted protein (19714.1 Da) accompanied by the small peaks of its oxidized forms (19730.1, 19746.1 and 19762.0 Da).

Conclusions

The adopted ESI MS approach allowed us to characterize in depth and comparatively the iron-binding properties of a single ferritin subunit. From the obtained ESI mass spectra we can infer that the metal clusters in the nucleation sites of HuLf are less labile than the di-iron center at the catalytic site of HuHf and ESI MS detectable. The low abundance of the iron-species in the ESI mass spectra of HuLf might be attributed to various non-mutually exclusive effects such as: i) an intrinsic instability of the metal center under the solution and ionization conditions required for the ESI MS experiment; ii) relevant cooperative effects in metal binding arising from the presence of other subunits, not yet identified in x-ray structures; iii) an overall deprotection of the inner surface upon disruption of the cage architecture. In any case, to the best of our knowledge, this is the first mass spectrometric evidence for the formation in solution of tetra- and octa-iron clusters mediated by the HuLf nucleation site, underscoring the relevance of these iron clusters for caged biomineral formation.

Author Contributions

The manuscript was written through the contributions of all authors. All authors have given approval to the final version of the manuscript.

Conflicts of interest

There are no conflicts to declare.

Acknowledgments

The authors thank AIRC and Fondazione Cassa Risparmio Firenze for funding the projects ‘‘Advanced mass spectrometry tools for cancer research: novel applications in proteomics, metabolomics and nanomedicine” (Multi-user Equipment Program 2016, grant number 19650). AP thanks Beneficentia Stiftung (Vaduz, Liechtenstein, BEN2020/34) and the University of Pisa (Rating Ateneo 2019-2020) for the financial support. The CIRCMSB (Consorzio Interuniversitario di Ricerca in Chimica dei Metalli nei Sistemi Biologici, Italy) is also acknowledged. L.C acknowledges Fondazione Cassa di Risparmio di Firenze (Bando ricerca scientifica 2019, project title “Development of ferritin-based nanodevices for the targeted delivery of drugs and imaging probes”) for a research grant. The authors acknowledge the financial support provided by the MIUR Grant “Progetto Dipartimenti di Eccellenza 2018-2022” to the Department of Chemistry “Ugo Schiff” of the University of Florence and the support and the use of resources of Instruct-ERIC, a landmark ESFRI project, and specifically the CERM/CIRMMP Italy centre.

Notes and references

1 P. Arosio, L. Elia and M. Poli, *IUBMB Life*, 2017, **69**, 414–422.

2 E. C. Theil, R. K. Behera and T. Tosha, *Coord. Chem. Rev.*, 2013, 257, 579–586.

3 B. Corsi, A. Cozzi, P. Arosio, J. Drysdale, P. Santambrogio, A. Campanella, G. Biasiotto, A. Albertini and S. Levi, *J. Biol. Chem.*, 2002, **277**, 22430–22437.

4 N. Surguladze, K. M. Thompson, J. L. Beard, J. R. Connor and M. G. Fried, *J. Biol. Chem.*, 2004, **279**, 14694–14702.

5 N. Surguladze, S. Patton, A. Cozzi, M. G. Fried and J. R. Connor, *Biochem. J.*, 2005, **388**, 731–740.

6 A. A. Alkhateeb and J. R. Connor, *Biochim. Biophys. Acta - Gen. Subj.*, 2010, **1800**, 793–797.

7 M. A. Knovich, J. A. Storey, L. G. Coffman, S. V. Torti and F. M. Torti, *Blood Rev.*, 2009, **23**, 95–104.

8 M. A. Kuiper, C. Mulder, G. J. van Kamp, P. Scheltens and E. C. Wolters, *J. Neural Transm. - Park. Dis. Dement. Sect.*, 1994, **7**, 109–114.

9 C. Pozzi, F. Di Pisa, C. Bernacchioni, S. Ciambellotti, P. Turano and S. Mangani, *Acta Crystallogr. Sect. D Biol. Crystallogr.*, 2015, **71**, 1909–1920.

10 C. Pozzi, S. Ciambellotti, C. Bernacchioni, F. Di Pisa, S. Mangani and P. Turano, *Proc. Natl. Acad. Sci. U. S. A.*, 2017, **114**, 2580–2585.

11 S. Ciambellotti, C. Pozzi, S. Mangani and P. Turano, *Chem. - A Eur. J.*, 2020, **26**, 5770–5773.

12 J. D. López-Castro, J. J. Delgado, J. A. Perez-Omil, N. Gálvez, R. Cuesta, R. K. Watt and J. M. Domínguez-Vera, *Dalt. Trans.*, 2012, **41**, 1320–1324.

13 A. Pratesi, D. Cirri, L. Ciofi and L. Messori, *Inorg. Chem.*, 2018, **57**, 10507–10510.

14 G. Tamasi, A. Carpini, D. Valensin, L. Messori, A. Pratesi, F. Scaletti, M. Jakupec, B. Keppler and R. Cini, *Polyhedron*, 2014, **81**, 227–237.

15 L. Messori, T. Marzo and A. Merlino, *J. Inorg. Biochem.*, 2015, **153**, 136–142.

16 A. Merlino, T. Marzo and L. Messori, *Chem. - A Eur. J.*, 2017, **23**, 6942–6947.

17 L. Massai, C. Zoppi, D. Cirri, A. Pratesi and L. Messori, *Front. Chem.*, 2020, **8**, 1–14.

18 C. Zoppi, L. Massai, D. Cirri, C. Gabbiani, A. Pratesi and L.

Messori, *Inorganica Chim. Acta*, 2021, **520**, 120297.
19 C. Zoppi, L. Messori and A. Pratesi, *Dalt. Trans.*, 2020, **49**, 5906–5913.
20 I. A. Kaltashov, C. E. Bobst and R. R. Abzalimov, *Protein Sci.*, 2013, **22**, 530–544.
21 S. Ciambellotti, A. Pratesi, G. Tassone, P. Turano, S. Mangani and C. Pozzi, *Chem. – A Eur. J.*, 2021, DOI:10.1002/chem.202102270.
22 M. Sengonul, J. Ruzicka, A. B. Attygalle and M. Libera, *Polymer (Guildf).*, 2007, **48**, 3632–3640.
23 L. D. Plath, A. Ozdemir, A. A. Aksenov and M. E. Bier, *Anal. Chem.*, 2015, **87**, 8985–8993.
24 W. ED, *Q. Rev. Biol.*, 1989, **64**, 261–290.
25 G. Kim, S. J. Weiss and R. L. Levine, *Biochim. Biophys. Acta - Gen. Subj.*, 2014, **1840**, 901–905.
26 R. L. Levine, L. Mosoni, B. S. Berlett and E. R. Stadtman, *Proc. Natl. Acad. Sci. U. S. A.*, 1996, **93**, 15036–15040.
27 J. C. Cutrin, D. Alberti, C. Bernacchioni, S. Ciambellotti, P. Turano, C. Luchinat, S. G. Crich and S. Aime, *Oncotarget*, 2018, **9**, 27974–27984.
28 D. Lalli and P. Turano, *Acc. Chem. Res.*, 2013, **46**, 2676–2685.